



OPEN High-temperature exposure during the early embryonic stage lowers core body temperature after growth via a hypothalamic *Igfbp2*-dependent mechanism

Yuki Yoshimura^{1✉}, Tatsuo Watanabe¹, Kazuomi Nakamura², Akira Futatsugi³, Katsuhiko Mikoshiba^{4,6} & Takeshi Y. Hiyama^{1,5✉}

The mechanisms underlying individual differences in core body temperature (T_c) are unexplained by genetic factors and poorly understood. Here, we investigated whether the environmental temperature during early development affects postnatal T_c . Mouse embryos were cultured from pronuclear to blastocyst stage in either standard (37 °C) or high (38 °C) temperature, and the T_c of each grown-up adult was measured. The adult 38 °C-incubated mice showed lower T_c than the 37 °C group without changes in activity levels. In the hypothalamus of the 38 °C group, insulin-like growth factor 1 (*Igf1*) and IGF binding protein 2 (*Igfbp2*) gene expression increased. The decrease in T_c in the wild-type 38 °C group was alleviated by brain neuron-specific *Igfbp2* knockout. This suggests that IGFBP2 binds to IGF-1 and, inhibits its binding to the receptor, thereby interfering with the thermogenic signaling of IGF-1. These results suggest that one of the factors determining individual postnatal T_c is the ambient temperature of embryos at an early developmental stage, which could affect epigenetic changes, such as DNA methylation, leading to alterations in the *Igf1* and *Igfbp2* gene expressions in adulthood.

Keywords Core body temperature, Insulin-like growth factor 1, IGF binding protein 2

The core body temperature (T_c) of homeotherms, including humans, fluctuates due to exercise and circadian rhythms, but it is constantly maintained around the individual's unique "set point" by the thermoregulatory system^{1,2}. The set point varies from person to person and decreases with age, but for both humans and mice, it generally falls within the range of 36.6 ± 0.5 °C^{3,4}. However, the mechanisms by which individual differences in T_c occur are poorly understood and cannot be explained solely by genetic factors. One study on birds suggested a connection between heat exposure to embryos and the T_c of the grown-up adults: in a study using Japanese quail (*Coturnix japonica*), incubation at a temperature 0.7 °C higher than the normal incubation temperature resulted in increased mitochondrial metabolism after birth⁵. Considering that mitochondrial metabolism in the preoptic area (POA) of the hypothalamus, which constitutes the central mechanism for thermoregulation (T_c), is involved in T_c control⁶, heat exposure during the embryonic stage may influence T_c regulation in adulthood.

POA sends inhibitory signals to mediate the differential inhibitory control of the sympatho-excitatory drive, determining brown adipose tissue (BAT) thermogenesis⁷. Thermosensitive neurons in the POA receive thermal signals from peripheral and deep-body thermoreceptors as well as hormonal and metabolic signals for the feedback control of T_c ⁸. Thus far, insulin-like growth factor-1 receptor (IGF-1R) is expressed in warm-sensitive neurons in the POA⁹. IGF-1R is a transmembrane tyrosine kinase receptor that receives insulin-like growth factor-1 (IGF-1) signaling. IGF-1 plays a crucial role in the central regulation of peripheral metabolism,

¹Department of Integrative Physiology, Tottori University Graduate School and Faculty of Medicine, Tottori University, 86 Nishi-cho, Yonago, Tottori 683-8503, Japan. ²Advanced Medicine, Innovation and Clinical Research Center, Tottori University Hospital, 36-1 Nishi-cho, Yonago, Tottori 683-8504, Japan. ³Department of Basic Medical Sciences, Kobe City College of Nursing, 3-4 Gakuen-nishi-machi, Nishi-ku, Kobe, Hyogo 651-2103, Japan. ⁴Shanghai Institute for Advanced Immunochemical Studies (SIAIS), ShanghaiTech University, Shanghai 201210, China. ⁵International Platform for Dryland Research and Education, Tottori University, 1390 Hamasaka, Tottori, Tottori 680-0001, Japan. ⁶Faculty of Science, Toho University, Miyama 2-2-1, Funabashi, Chiba 274-8510, Japan. ✉email: yoshimura@tottori-u.ac.jp; hiyama@tottori-u.ac.jp

and administration of IGF-1 to the POA induces dose-dependent hyperthermia⁹. The POA sends inhibitory signals through distinct pathways to other hypothalamic nuclei, such as the dorsomedial hypothalamus (DMH) and raphe pallidus (RPa), to mediate differential inhibitory control of the sympathoexcitatory drive that drives brown adipose tissue (BAT) thermogenesis¹⁰. IGF-1 can affect the activity of preoptic GABAergic inhibitory neurons projecting to the DMH and RPa, leading to disinhibition of the sympathoexcitatory drive and resulting in BAT activation and subsequent hyperthermia⁹.

Heatwave exposure during early pregnancy is likely to increase the risk of stillbirth¹¹. Processes critical to embryonic development such as cell proliferation, migration, differentiation, and programmed cell death (apoptosis) are adversely affected by elevated maternal temperatures¹². Heat exposure can cause irreversible changes in embryonic development and it cannot be ruled out that these effects may influence postnatal development and physiological functions of grown-up adults. Many studies have supported the hypothesis that there is a link between the periconceptual, fetal, and early infant phases of life and the long-term development of metabolic disorders; this hypothesis is known as the developmental origins of the health and disease (DOHaD) hypothesis¹³. An abnormal nutritional environment around the embryo, which may cause detrimental changes in embryonic development, can also affect the long-term physiological functions of adults^{14,15}. Malnutrition during gestation, such as suboptimal maternal nutrition, increases the risk of late-life diseases, such as hypertension and type 2 diabetes^{16–18}. In a rat study, pre-implantation maternal low-protein diets increased body weight and systolic blood pressure in male offspring¹⁹. We hypothesized that the thermal environment of early embryos could, like nutritional conditions, influence the long-term physiological functions of grown-up adults.

In this study, we investigated the effect of incubation temperature for early-stage embryos on the T_c of the grown-up adult mice. To this end, mouse in vitro fertilized embryos were cultured from the pronuclear stage to the blastocyst stage at either standard body temperature (37 °C group) or high temperature (38 °C group), and the T_c of each grown-up adult was measured. We could not test the low temperature condition, because most 36 °C-incubated embryos were lethal. The adult 38 °C group showed lower T_c than the 37 °C group without altering activity levels. Quantitative polymerase chain reaction (qPCR) analysis of hypothalamic tissues for candidate genes that could be responsible for the determination of T_c revealed enhanced expression of IGF-1 and insulin-like growth factor binding protein-2 (IGFBP2), which bind to and disturb the binding of IGF-1 to its receptor (IGF-1R)^{20,21}. Brain neuron-specific *Igfbp2* conditional knockout (cKO) mice showed an amelioration of the T_c reduction in the 38 °C group, suggesting that increased expression of IGFBP2 in the hypothalamus in the 38 °C group caused the reduction of T_c after growth by disturbing the Igf-1 signaling in the hypothalamus of mice.

Material and methods

Animals

The experimental protocols were approved by the Safety Committee for Recombinant DNA Experiments at Tottori University (35-071, 2024-010) and the Committee on the Ethics of Animal Experiments in Tottori University Faculty of Medicine (22-Y-6, and 23-Y-45), and were carried out following the Guidelines for Animal Experiments at Tottori University. All experiments described here conform to the ARRIVE guidelines. All mice (C57BL/6N and ICR strains) were purchased from Japan SLC (Tokyo, Japan). The *CaMK2a-Cre* transgenic mouse strain (B6.Cg-Tg(Camk2a-cre)20Kmik/KmikRbrc, RBRC00254) was provided by the RIKEN BRC through the National BioResource Project of MEXT/AMED, Japan²². The *Igfbp2*-floxed mouse line was generated as described follows in “Generation of *Igfbp2*-floxed mouse”. They were housed in individual plastic cages [24.5 × 17.5 × 12.5 cm; (length × width × depth)] with wood-chip bedding in a room maintained at 25 ± 1 °C. They experienced a photoperiod of 12 h light:12 h dark, with lights on at 0700 h. All mice had ad libitum access to water and standard laboratory chow.

Mouse embryo in vitro culture

We established a mammalian animal model to validate the influence of the mother's T_c on offspring. Here, we used mouse reproductive technologies such as in vitro fertilization, embryo culture, and embryo transfer into the uterus. We cultured in vitro mouse fertilized zygotes from the pronuclear stage to the blastocyst stage at 37 °C (37 °C group); standard culture temperature, or 38 °C (38 °C group) with CO₂ incubators (Fig. 1). Briefly, C57BL/6N female mice of 3-weeks old were peritoneally injected with 5 IU/mouse pregnant mare's serum (Serotropin, ASKA Animal Health, Japan), followed by 5 IU/mouse hCG (Gestron, Kyoritsu Seiyaku, Japan) injection for superovulation that occurred 48 h later. Eggs obtained from superovulated mice sacrificed by cervical dislocation were fertilized in vitro with C57BL/6N sperm in HTF medium (ARK Resource, Japan). The time course of embryo culture in KSOM medium (ARK Resource, Japan) is shown in Fig. 1. After fertilization was confirmed, fertilized zygotes were divided equally and randomly into the two groups, 37 °C and 38 °C groups, cultured in vitro to develop to the blastocyst stage in a CO₂ incubator at either 37 or 38 °C. The embryos were transferred to the uteri of pseudo-pregnant ICR mice chosen randomly. After birth, 9-week-old male mice were subjected to body temperature and gene-expression analyses.

Measurement of T_c and samplings of the hypothalamus and the liver

T_c was measured using a biotelemetry system (Data Science International [DSI], MN; Lange et al., 1991). In brief, mice were anesthetized by the inhalation of 5% isoflurane, and a battery-operated transmitter (TA11TA-F10, DSI) was implanted intraperitoneally (i.p.). After a 1-week-recovery period, the T_c and physical levels were measured for another two weeks. Data were obtained from the last 7 days. The area under the curve (AUC) was calculated as the integral value of T_c . After cessation of measurement, the mice were anesthetized with M/M/B consisting of medetomidine (Domitor, Nippon Zenyaku Kogyo, Japan), midazolam (Midazolam Injection, Sandoz, Japan), and butorphanol (Vetorphale, Meiji Seika Pharma, Japan) at doses of 0.3, 4, and 5 mg/kg body

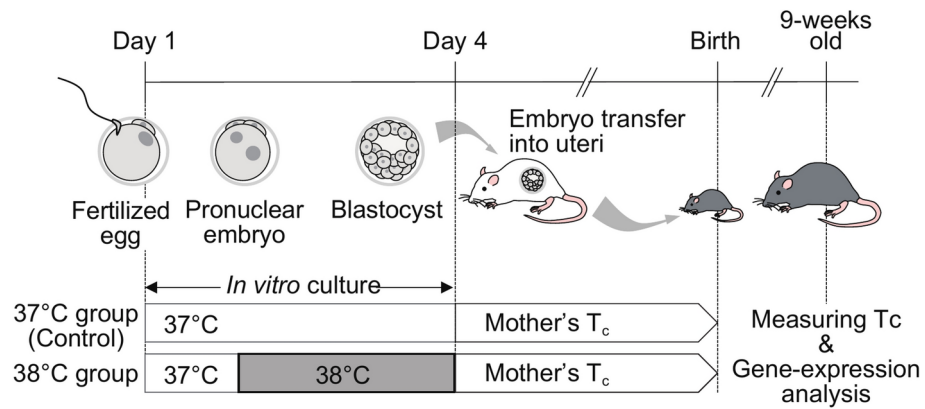


Fig. 1. Experimental workflow.

weight, respectively²³. The whole body was perfused with 25 mL of cold saline using a microsyringe pump (CXF-101, ISIS, Japan). The hypothalamus and liver were immediately removed and frozen in liquid nitrogen. The samples were kept at -80°C for molecular analysis.

qPCR analysis for candidate genes, *Igf1* and *Igfbp2*

Igf1 and *Igfbp2* mRNA expression levels in the hypothalamus and liver were analyzed using qPCR. The tissue was homogenized at 4°C with a multi-beads shaker (MB2200, Yasui Kikai, Japan), and mixed with RNase-free water (W1503, Merck, Germany) and ISOGEN II (311-07361, NIPPON GENE, Japan). After centrifugation (12,000 rpm, 15 min, 4°C), the supernatant was collected and mixed with an equal volume of isopropanol (166-04836, FUJIFILM Wako Pure Chemical, Japan). The RNA pellet was washed twice with 75% ethanol, then dissolved in RNase-free water after a brief air drying. Total RNA was reverse-transcribed using a high-capacity cDNA reverse transcription kit with an RNase inhibitor (4374966; Thermo Fisher Scientific). The cDNA was diluted 5 times with RNase water before qPCR. qPCR was performed using the PowerUp SYBR Green Master Mix (A25742; Thermo Fisher Scientific). The qPCR primers used are listed in Supplementary Table 1.

Generation of *Igfbp2*-floxed mouse

Igfbp2-floxed mice were generated by the standard protocol for gene editing technology, CRISPR/Cas9 system²⁴. Briefly, two crRNAs (crRNA1 and crRNA2) and two ssDNAs (ssDNA1 and ssDNA2) were synthesized as shown in Supplemental Table 2 (Alt-R[®] CRISPR-Cas9 crRNA and Ultramer[®] DNA Oligo, respectively; Integrated DNA Technologies [IDT], IA). Before micro-injection, 2 ng/ μL of crRNAs, 8 ng/ μL of Alt-R[®] CRISPR-Cas9 tracrRNA (1072532, IDT), 50 ng/ μL of Alt-R[®] S.p. Cas9 Nuclease V3 (1081058, IDT), and 100 ng/ μL of ssDNAs were mixed in sterilized water for the embryo (W1503, Merck), and filtrated with Ultrafree-MC (UFC30GV25, Merck). The filtered mixture was microinjected into the pronuclei and cytoplasm of the fertilized zygotes obtained from C57BL/6N female mice. The next day, the injected zygotes were transferred into the oviducts of pseudo-pregnant ICR mice. After birth, the genotypes of the pups were identified by genomic PCR and sequence analysis of the floxed region. Briefly, genomic PCR was performed using KOD FX Neo (KFX-201, TOYOBO, Japan) using a standard procedure. The genotyping primers used are listed in Supplementary Table 2. The product of genomic PCR was purified with the Wizard[®] SV Gel and PCR Clean-Up System (A9281, Promega, WI), and sequenced with the Value Read DNA sequence (Eurofins Genomics, Japan). *Igfbp2*-floxed mice were mated with *CaMK2a-Cre* transgenic mice to generate neuron-specific *Igfbp2* cKO mice. The *CaMK2a* gene was also expressed in the testes, so we used *Igfbp2* cKO (*Igfbp2*^{lox/-}::*CaMK2a-Cre*) and the control mice (*Igfbp2*^{+/-}::*CaMK2a-Cre*), which are the offspring of male F1 mice of *Igfbp2*-flox and *CaMK2a-Cre* mice, respectively. Notably, both *Igfbp2* cKO and control mice harbored the *CaMK2a-Cre* transgene.

Igfbp2 cKO male mice were subjected to T_c and physical levels analyses, as described above. Briefly, the embryo culture was performed at 38°C . After birth, the control and *Igfbp2* cKO mice were identified by genotyping. The mice which were obviously small and weak (the body weight at 4 weeks old was under 15 g), or which had an system error at measuring the T_c were omitted. To confirm the reduction in *Igfbp2* expression in *Igfbp2* cKO mice, tissues from control and *Igfbp2* cKO mice were collected and frozen quickly. After homogenization with a multi-beads shaker, RNA was purified using the FastGene RNA Premium Kit (FG-81050, Nippon Genetics, Japan). Total RNA was reverse-transcribed and cDNA was used for qPCR, as described above.

Statistical analysis

All results are expressed as mean \pm S.E.M. Data were analyzed for statistical significance using a Student's t-test after Shapiro-wilk and Levene tests to assess the normality and the equal variances, respectively; when the latter two tests failed to confirm those variables, data were analyzed by Mann-Whitney U tests. These tests were performed using the R software (version 2023.12.0 + 369)²⁵. Differences were considered statistically significant at $p < 0.05$.

Results

High ambient temperature at an early embryonic stage causes low T_c after growth

Daily changes of T_c and activity were measured on both 37 °C and 38 °C groups of mice at the same age (9-weeks old; Fig. 1). Both groups showed similar diurnal rhythm of T_c (Fig. 2a) and physical activity (Fig. 2b). However, the T_c of the 38 °C group was lower than that of the 37 °C group (Fig. 2a). AUC of T_c indicated a significant difference in T_c from Zeitgeber time (ZT) 3 to ZT12 between the two groups (Fig. 2c), while there were no significant differences in the activities during the same period (Fig. 2d).

High ambient temperature causes upregulation of hypothalamic *Igf1* and *Igfbp2* expressions

To test the possibility that thermogenic signaling through IGF-1 underlies the T_c changes in the 38 °C group, we examined the gene expression levels of IGF-1, its binding proteins (IGFBP2 and 5), and its receptors (IGF-1R, and insulin receptor [INSR]) in the grown-up adult of both groups. IGFBP2 and 5 are reported to be expressed in the brain^{26–28}. Gene expression analysis by qPCR revealed that hypothalamic *Igf1* and *Igfbp2* mRNA expression was upregulated in the 38 °C group, without any changes in hepatic expression (Fig. 3a,b). The expression levels of *Igfbp5* and its receptors (*Igf1r* and *Insr*) did not differ between the two groups (Fig. 3c, d,e). As IGFBP2

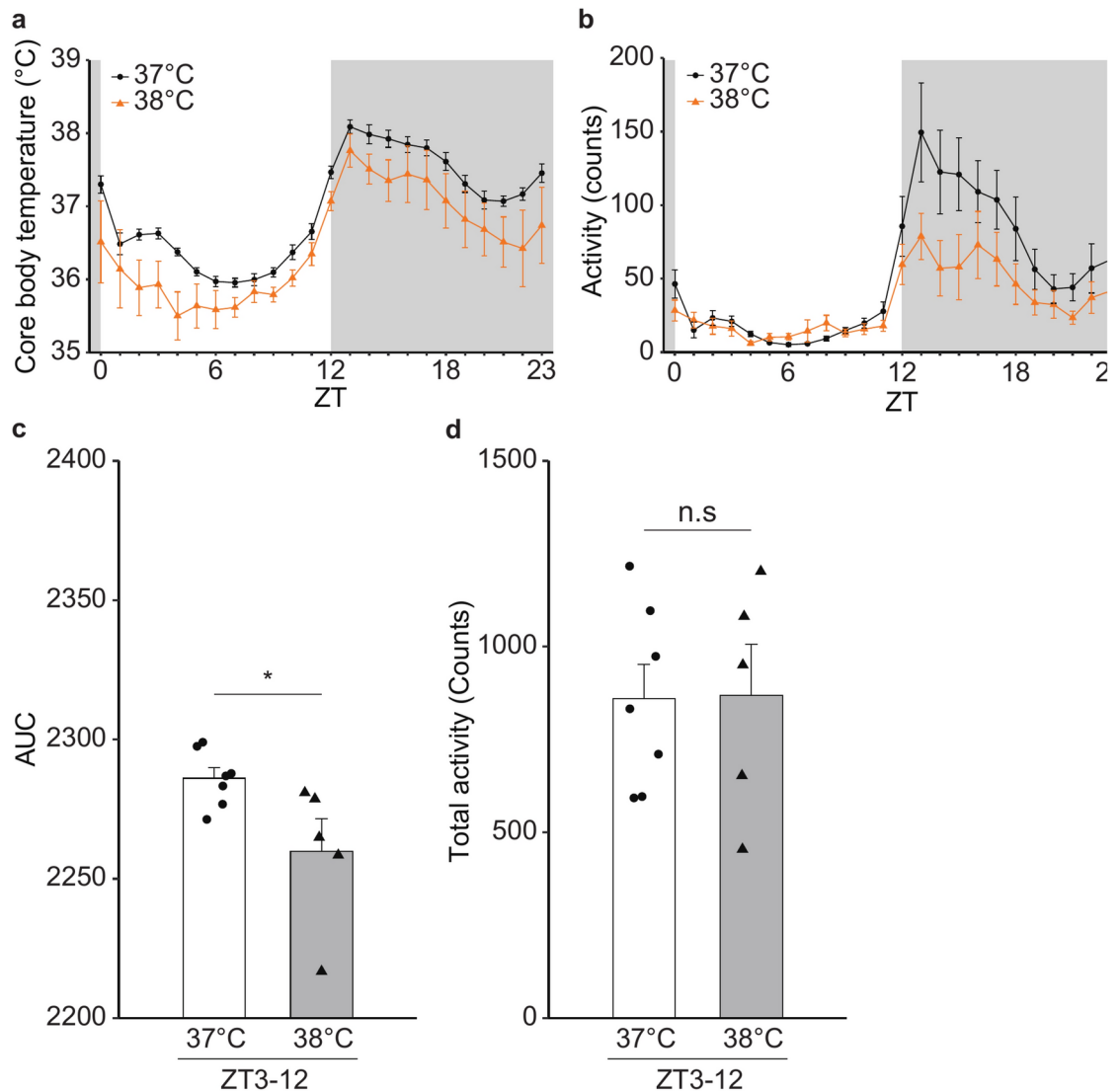


Fig. 2. Effect of environmental temperature near mouse embryos at the early stage on the T_c of the grown-up male mice. (a, b) Circadian rhythms of core body temperature (a) and activity (b) of the male WT mice (n=7; 37 °C group, n=5; 38 °C group). For a given mouse, data were obtained every 1 h for 7 days (see Material and Methods), followed by calculation of a 7-day mean of the data at each time-point. Subsequently, we obtained a mean value (namely, ● and ▲ shown in Fig. 2a and b) at each time-point for a given group. The error bar shows standard error of the mean (SEM). (c) Area under the curve (AUC) of the temperature changes from ZT3 to ZT12. Error bar shows SEM. * p -value < 0.05 (Student's t -test). (d) Total activity from ZT3 to ZT12. Error bar shows SEM.

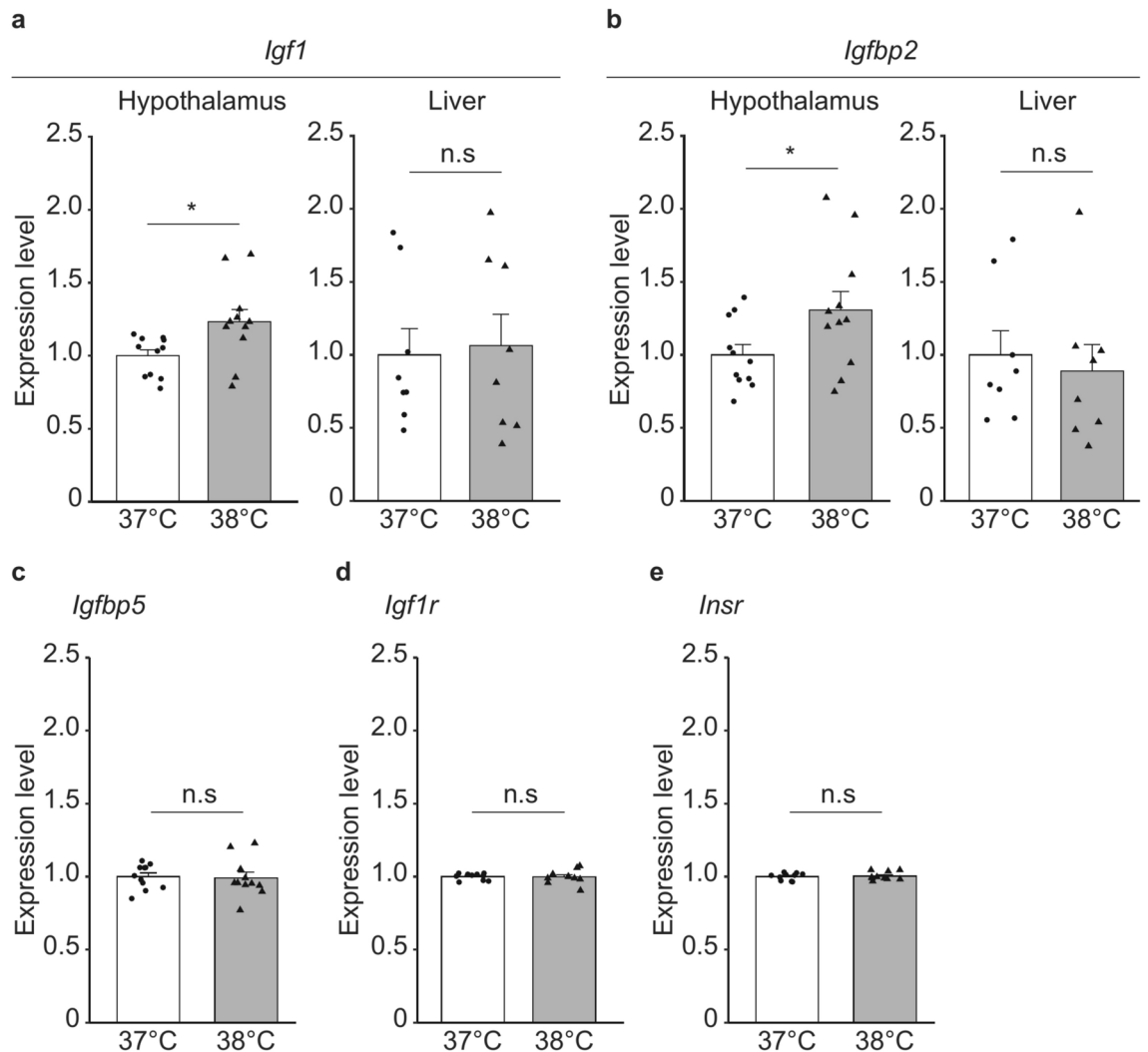


Fig. 3. Effect of the environmental temperature near mouse embryos at the early stage on the *Igf1* and *Igfbp2* expressions in the hypothalamus and liver and the *Igfbp5*, *Igf1r* and *insr* in the hypothalamus of the grown-up male mice. (a) Expression level of *Igf1* mRNA in the hypothalamus (n = 10 in each of the 37 °C and 38 °C groups) and liver (n = 8 in each group). Error bar shows SEM. * *p*-value < 0.05 (Student's *t*-test). (b) Expression level of *Igfbp2* mRNA in the hypothalamus (n = 11 in each of the 37 °C and 38 °C groups) and liver (n = 8 in each group). Error bar shows SEM. * *p*-value < 0.05 (Student's *t*-test). (c) Expression level of *Igfbp5* mRNA in the hypothalamus (n = 11 in each of the 37 °C and 38 °C groups). Error bar shows SEM. (d) Expression level of *Igf1r* mRNA in the hypothalamus (n = 10 in each of the 37 °C and 38 °C groups). Error bar shows SEM. (e) Expression level of *Insr* mRNA in the hypothalamus (n = 10 in each of the 37 °C and 38 °C groups). Error bar shows SEM.

disturbs the binding of IGF-1 to its receptors, these data suggest that increased expression of IGFBP2 caused a reduction in the thermogenic function of IGF-1 and lowered the T_c of the 38 °C group.

Generation of brain neuron-specific *Igfbp2* cKO mouse

To test our hypothesis that *Igfbp2* mediates the T_c reduction in the 38 °C group, we next generated an *Igfbp2* conditional knockout mouse line. As IGFBP2 and IGF-1 are present not only in the brain, but also in the liver of vertebrates, including mice^{29,30}, we generated an *Igfbp2* floxed mouse line using the CRISPR/Cas9 system. Figure 4a shows the construction of the *Igfbp2* floxed mouse, in which two loxP sites were inserted in *Igfbp2* intron 1 and the downstream of the 3' UTR, respectively. The insertion of loxP sequences into the proper target position in *Igfbp2* floxed mouse was confirmed by DNA sequence analysis (Fig. 4b). To generate a brain neuron-specific *Igfbp2* cKO, *Igfbp2* floxed mice were mated with *CaMK2a-Cre* transgenic mice, in which *Cre* recombinase is expressed specifically in brain neurons. In the F1 mouse with the *Igfbp2* floxed allele and *CaMK2a-Cre* transgene, the *Igfbp2* KO allele was detected in the hypothalamus, but not in the liver, indicating that a brain-specific *Igfbp2* cKO mouse was established (Fig. 4c and Supplemental Fig. S1).

In the following study, we used *Igfbp2*^{+/±}::*CaMK2a-Cre* mice as the control, in which *Igfbp2* allele is half that of the wild type, because the *CaMK2a-Cre* gene is also expressed in the testis, and we could not obtain

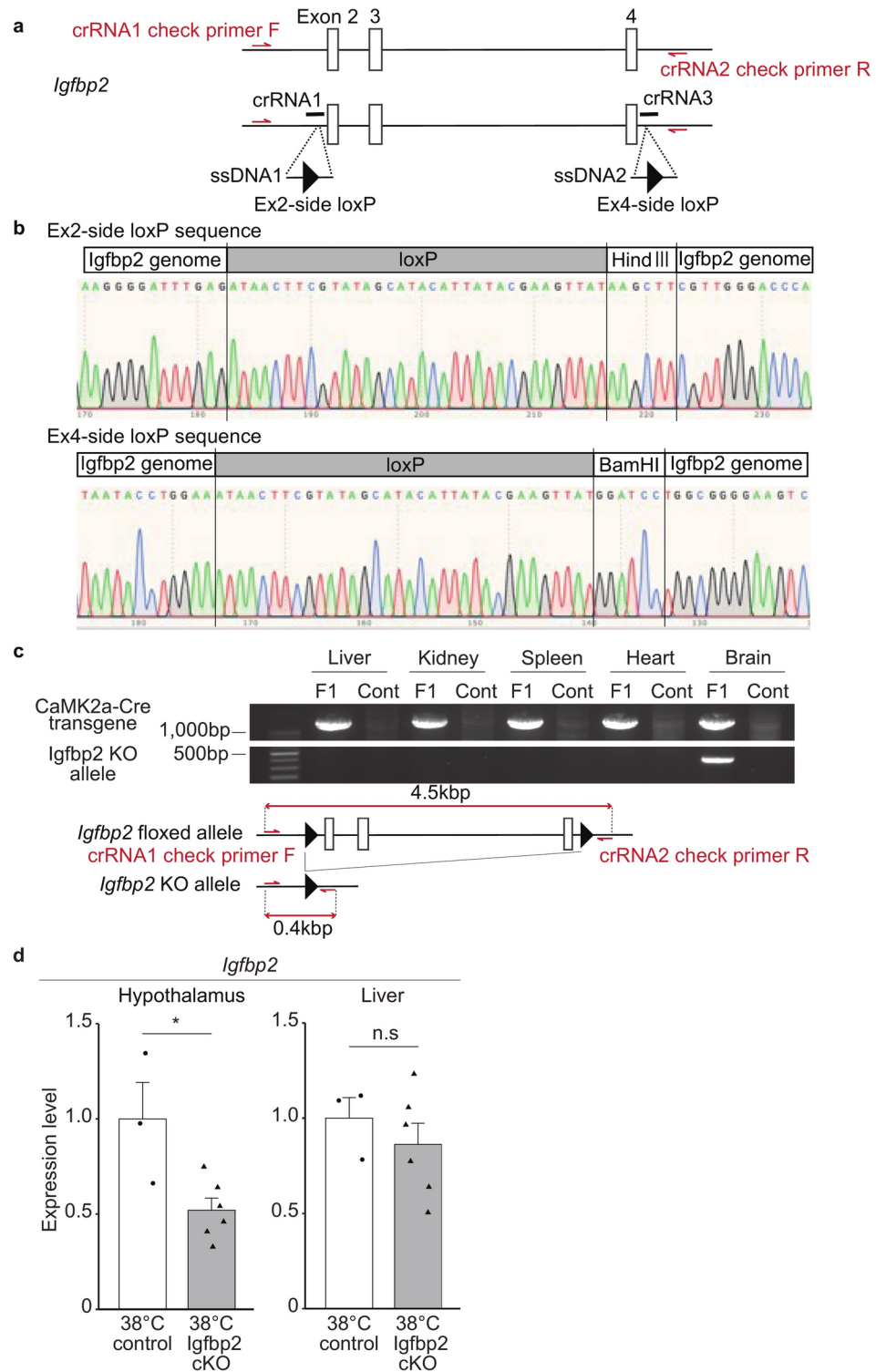


Fig. 4. Generation of brain-specific *Igfbp2* knock-out (*Igfbp2* cKO) mouse. **(a)** Construction of *Igfbp2*-floxed mouse. Red arrows show the genotyping primers, crRNA1 check primer F, and crRNA2 check primer R in Supplemental Table 2, to detect the *Igfbp2* KO allele. **(b)** Sequence analysis to confirm the loxP knock-in. **(c)** PCR results to detect the *Igfbp2* KO allele by Cre/loxP recombination. F1 mouse is *Igfbp2*^{+/lox}::*CaMK2a-Cre*, and the cont is the *Igfbp2*^{+/lox} mouse as a control. Bottom schema shows the construction of *Igfbp2* KO allele primers. **(d)** Expression level of the *Igfbp2* mRNA in the hypothalamus and liver of the male *Igfbp2* cKO (n = 6) and the control mice (n = 3) exposed to 38 °C at their early stage of the embryo. Error bar shows SEM. * *p*-value < 0.05 (Student's *t*-test).

Igfbp2^{fl^{ox}/fl^{ox}::CaMK2a-Cre mice. In the cKO (*Igfbp2*^{fl^{ox}/-::CaMK2a-Cre) mice, IGFBP2 expression is expected to be null, specifically in neurons in the brain, and half of the wild type in other regions, including the liver. We confirmed that the *Igfbp2* expression level in *Igfbp2* cKO mice after growth was specifically decreased in the hypothalamus, but not in the liver (Fig. 4d).}}

Brain neuron-specific knockout of *Igfbp2* mitigated the T_c reduction in the 38 °C group

The *Igfbp2* cKO and the control mice showed indistinguishably the same circadian rhythm of T_c and activity when they were born from natural breeding (Supplemental Fig. S2), indicating that brain neuron-specific deletion of *Igfbp2* does not modify the T_c . The T_c rhythm of control mice (*Igfbp2*^{+/+::CaMK2a-Cre mice) in Supplemental Fig. S2a was comparable to that of the WT 37 °C group (shown in Fig. 2a).}

Next, we examined the mice that suffered 38 °C exposure (38 °C *Igfbp2* cKO and 38 °C control). Both groups exhibited typical circadian rhythms for T_c and activity (Fig. 5a,b). The T_c rhythm of control mice in Fig. 5a was comparable to that of the WT 38 °C group (shown in Fig. 2a). Notably, both control (*Igfbp2*^{+/+::CaMK2a-Cre mice) and WT mice showed diurnal T_c changes between ~35.5 and ~37.5 °C, indicating that halving the expression of IGFBP2 throughout the body does not affect the T_c reductions by embryonic 38 °C incubation.}

In the 38 °C *Igfbp2* cKO mice, however, the T_c was higher than in the 38 °C control group during the latter half of the day and night time (Fig. 5a, ZT 3–12 and 19–23, respectively). The AUCs of the 38 °C *Igfbp2* cKO group were significantly higher than those of the 38 °C control mice in these time periods, suggesting that IGFBP2 in the hypothalamus neurons is critical for the T_c reduction by the heat exposure at early stages (Fig. 5c). In contrast, while the overall cKO activity appeared to be low, there were no significant differences in activity between the two groups during the same period (Fig. 5b,d). Notably, the cKO mice had no different body weight (at 8 weeks of the age) comparing to the control group with a shared genetic background, indicating that the T_c difference between cKO and control mice (at 9 weeks of the age) may not be due to differences in body mass (Fig. 5e).

Discussion

Here, a rise by 1 °C in the environmental temperature (i.e. 38 °C vs 37 °C) around embryos led to a decrease in T_c of the grown-up adult. Since there was no significant difference in the activities between the two groups, thermosensory and/or thermoeffector pathways as well as function of the thermoregulatory center might have undergone alterations by the early exposure to 38 °C. In this study, significant differences in T_c were observed during the daytime (ZT3–12), which corresponds to the sleeping period for mice (Figs. 2 and 5). This result may support our notion that the difference in body temperature is due to some changes in metabolic functions rather than behavioral activities. Expressions of *Igf1* and *Igfbp2* mRNAs in the hypothalamus of the 38 °C group were upregulated. IGFBP2 induced by heat exposure, inhibits IGF-1 function in the POA of the hypothalamus; this inhibitory effect exceeds the thermogenic action of IGF-1, resulting in a decrease in T_c . The hypothesis is supported by the increases in T_c in the present *Igfbp2* cKO mice exposed to 38 °C at their early stage of the embryo, as compared with the 38 °C control mouse T_c . Importantly, the increase in T_c was observed only in the 38 °C-incubated *Igfbp2* cKO but not in the *Igfbp2* cKO born from natural breeding, confirming that this IGFBP2-mediated mechanism works only when the mice receive heat exposure at early embryonic stage.

Malnutrition during gestation to a decrease in maternal nutrition leads to low birth weight, and it is correlated with the development of metabolic diseases such as type 2 diabetes³¹. In such cases, the mismatch between normal and sufficient postnatal nutrition following poor intrauterine nutrition accelerates weight gain, leading to glucose intolerance, insulin resistance and lipid accumulation^{32,33}. Our mice of the 38 °C group might have undertaken such adaptive changes in the thermoregulatory system to cope with the high environmental temperature at the early stage of the embryos. However, this possibility needs to be tested in future study. Another possibility is that some studies have revealed the involvement of epigenetics in postnatal weight gain and elevated systolic blood pressure in adults, owing to maternal malnutrition before implantation^{19,34}. It is also reported that the epigenetic modification affects the *Igfbp2* expression level. Kammel et al. showed that the DNA methylation of the hepatic *Igfbp2* expression level in infants has the relationship with the fatty liver³⁵. According to McDonald's group, IGFBP2 expression correlated the glioma with necrosis and microvascular proliferation, whose prognosis is relatively poor³⁶. Zheng et al.³⁷ reported that IGFBP2 expression had the association with DNA methylation in glioma. Therefore, we should investigate the role of epigenetics in the decrease in T_c of the present 38 °C group, as well.

In most mammals, fertilization and embryo growth occur in the uterus, which is located deep inside dams. Therefore, it is difficult to manipulate the intrauterine temperature (T_{uterus}). For example, try to increase the T_{uterus} could go wrong, because the thermoregulatory system of dams would take action to lower the increased T_c induced by the change in the T_{uterus} . Even if the T_{uterus} is maintained constant by experimental devices, changes in several physiological systems, such as the nervous and endocrine systems, may be induced, leading to effects other than the temperature itself exerted on the embryo. Therefore, we used mouse reproductive technologies. This allowed us to culture the mouse embryos in vitro in a CO₂ incubator before conception. Embryos were transferred into the uteri of pseudo-pregnant ICR mouse after in vitro culturing. To examine the effects of environmental temperature changes on the embryo and/or fetus during the entire pregnant period, the generation of transgenic and/or knockout pregnant mice with hyperthermia would be one option. As the upregulation of uncoupling protein (UCP) in the mitochondria of brown adipose tissue results in an increase in heat production, UCP could be a target molecule³⁸. Currently, some transgenic animals with hypothermia are available³⁹. It would be interesting to examine the effect of maternal hypothermia on the T_c of the grown-up adults.

In this study, we generated *Igfbp2* cKO mice and used them to analyze T_c controls. Considering the inhibitory effect of IGFBP2 on IGF-1, this mouse line may have other phenotypes, such as those related to the neuroendocrine system. One possible candidate is the growth hormone (GH)/IGF-1 axis⁴⁰. *Igf-1* null mice

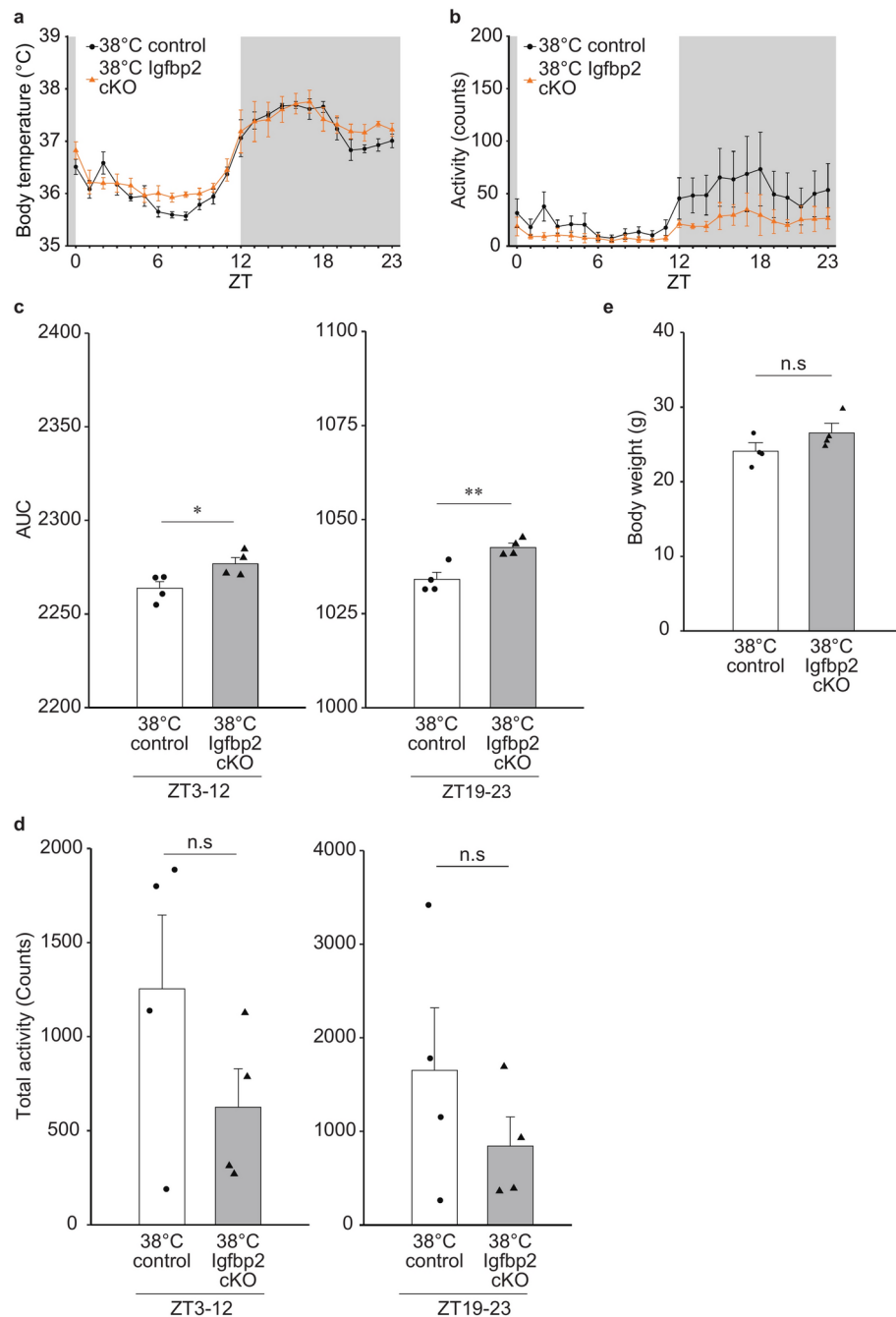


Fig. 5. Effect of cKO of brain *Igfbp2* on T_c of adult mice exposed to the environmental temperature of 38 °C at their early stage of embryos. **(a, b)** Circadian rhythms of T_c **(a)** and activity **(b)** of the male *Igfbp2* cKO and the control mice ($n = 4$ in each group) exposed to 38 °C at their early stage of embryo. Error bar shows SEM. **(c)** AUC of the temperature changes from ZT3 to ZT12 and ZT19 to ZT23. Error bar shows SEM. * p -value < 0.05 (Student's t-test). ** p -value < 0.01 (Student's t-test). **(d)** Total activity (counts) from ZT3 to ZT12 and ZT19 to ZT23. Error bar shows SEM. **(e)** Body weight of 8-weeks old *Igfbp2* cKO mice exposed to the environmental temperature of 38 °C at their early stage of the embryo. *Igfbp2* cKO and the control mice ($n = 4$ in each group) were used. Error bar shows SEM.

exhibit retarded growth after birth⁴¹. At an early postnatal age (4 weeks old), *Igfbp2* cKO mice gained slightly more weight than control mice (data not shown), though the difference disappeared until 8 weeks old (Fig. 5e). Since the gene deletion was performed specifically in the brain, it is possible to consider that brain IGF-1 might activate growth hormone-releasing hormone (GRH) and/or inhibit somatostatin neurons in the hypothalamus, leading to the activation of the GH/IGF-1 axis and weight gain. *Igfbp2* cKO is a useful animal model for the analysis of brain development in the GH/IGF-1 axis.

The mechanisms by which individual differences in T_c arise cannot be fully explained by genetic factors alone and are poorly understood. The results of this study demonstrate for the first time that embryos exposed to a high-temperature environment during early development, such as when the mother has a high fever in early pregnancy, tend to have a lower T_c after birth. Furthermore, this mechanism is thought to involve the inhibition of IGF-1-mediated thermogenic signaling in the POA by IGFBP2. We propose that this is a possible mechanism by which individual differences in T_c arises depending on maternal T_c during early pregnancy. This mechanism may provide a clue as to why the T_c of mammals is approximately 37 °C and not some other temperature.

Data availability

The datasets used and/or analyzed during the current study available from the corresponding author on reasonable request.

Received: 8 August 2024; Accepted: 18 November 2024

Published online: 03 December 2024

References

1. Tan, C. L. & Knight, Z. A. Regulation of body temperature by the nervous system. *Neuron* **98**, 31–48. <https://doi.org/10.1016/j.neuron.2018.02.022> (2018).
2. Hammel, H. T. Regulation of internal body temperature. *Annu. Rev. Physiol.* **30**, 641–710. <https://doi.org/10.1146/annurev.ph.30.030168.003233> (1968).
3. Waalen, J. & Buxbaum, J. N. Is older colder or colder older? The association of age with body temperature in 18,630 individuals. *J. Gerontol. A Biol. Sci. Med. Sci.* **66**, 487–492. <https://doi.org/10.1093/geronol/glr001> (2011).
4. Reitman, M. L. Of mice and men - environmental temperature, body temperature, and treatment of obesity. *FEBS Lett.* **592**, 2098–2107. <https://doi.org/10.1002/1873-3468.13070> (2018).
5. Stier, A., Monaghan, P. & Metcalfe, N. B. Experimental demonstration of prenatal programming of mitochondrial aerobic metabolism lasting until adulthood. *Proc. Biol. Sci.* **289**, 20212679. <https://doi.org/10.1098/rspb.2021.2679> (2022).
6. Guimaraes, N. C. et al. Mitochondrial pyruvate carrier as a key regulator of fever and neuroinflammation. *Brain Behav. Immun.* **92**, 90–101. <https://doi.org/10.1016/j.bbi.2020.11.031> (2021).
7. Morrison, S. F. & Nakamura, K. Central mechanisms for thermoregulation. *Annu. Rev. Physiol.* **81**, 285–308. <https://doi.org/10.1146/annurev-physiol-020518-114546> (2019).
8. Tabarean, I. Central thermoreceptors. *Handb. Clin. Neurol.* **156**, 121–127. <https://doi.org/10.1016/B978-0-444-63912-7.00007-2> (2018).
9. Sanchez-Alavez, M. et al. Insulin-like growth factor 1-mediated hyperthermia involves anterior hypothalamic insulin receptors. *J. Biol. Chem.* **286**, 14983–14990. <https://doi.org/10.1074/jbc.M110.188540> (2011).
10. Nakamura, K. & Morrison, S. F. A thermosensory pathway that controls body temperature. *Nat. Neurosci.* **11**, 62–71. <https://doi.org/10.1038/nn2027> (2008).
11. Wang, J., Tong, S., Williams, G. & Pan, X. Exposure to heat wave during pregnancy and adverse birth outcomes: An exploration of susceptible windows. *Epidemiology* **30**(Suppl 1), S115–S121. <https://doi.org/10.1097/EDE.0000000000000995> (2019).
12. Edwards, M. J., Saunders, R. D. & Shiota, K. Effects of heat on embryos and fetuses. *Int. J. Hyperthermia* **19**, 295–324. <https://doi.org/10.1080/0265673021000039628> (2003).
13. Lacagnina, S. The developmental origins of health and disease (DOHaD). *Am. J. Lifestyle Med.* **14**, 47–50. <https://doi.org/10.1177/1559827619879694> (2020).
14. Barker, D. J. In utero programming of chronic disease. *Clin. Sci.* **95**, 115–128 (1998).
15. Grilo, L. F. et al. Metabolic disease programming: From mitochondria to epigenetics, glucocorticoid signalling and beyond. *Eur. J. Clin. Invest.* **51**, e13625. <https://doi.org/10.1111/eci.13625> (2021).
16. Tarry-Adkins, J. L. & Ozanne, S. E. Nutrition in early life and age-associated diseases. *Ageing Res. Rev.* **39**, 96–105. <https://doi.org/10.1016/j.arr.2016.08.003> (2017).
17. Barker, D. J., Osmond, C., Golding, J., Kuh, D. & Wadsworth, M. E. Growth in utero, blood pressure in childhood and adult life, and mortality from cardiovascular disease. *BMJ* **298**, 564–567. <https://doi.org/10.1136/bmj.298.6673.564> (1989).
18. Ravelli, A. C. et al. Glucose tolerance in adults after prenatal exposure to famine. *Lancet* **351**, 173–177. [https://doi.org/10.1016/S0140-6736\(97\)07244-9](https://doi.org/10.1016/S0140-6736(97)07244-9) (1998).
19. Kwong, W. Y., Wild, A. E., Roberts, P., Willis, A. C. & Fleming, T. P. Maternal undernutrition during the preimplantation period of rat development causes blastocyst abnormalities and programming of postnatal hypertension. *Development* **127**, 4195–4202. <https://doi.org/10.1242/dev.127.19.4195> (2000).
20. Binkert, C., Landwehr, J., Mary, J. L., Schwander, J. & Heinrich, G. Cloning, sequence analysis and expression of a cDNA encoding a novel insulin-like growth factor binding protein (IGFBP-2). *EMBO J.* **8**, 2497–2502. <https://doi.org/10.1002/j.1460-2075.1989.tb08386.x> (1989).
21. Russo, V. C., Rekaris, G., Baker, N. L., Bach, L. A. & Werther, G. A. Basic fibroblast growth factor induces proteolysis of secreted and cell membrane-associated insulin-like growth factor binding protein-2 in human neuroblastoma cells. *Endocrinology* **140**, 3082–3090. <https://doi.org/10.1210/endo.140.7.6771> (1999).
22. Nakayama, K. et al. RNG105/caprin1, an RNA granule protein for dendritic mRNA localization, is essential for long-term memory formation. *Elife* **6**, 29677. <https://doi.org/10.7554/eLife.29677> (2017).
23. Kawai, S., Takagi, Y., Kaneko, S. & Kurosawa, T. Effect of three types of mixed anesthetic agents alternate to ketamine in mice. *Exp. Anim.* **60**, 481–487. <https://doi.org/10.1538/expanim.60.481> (2011).
24. Horii, T. et al. Efficient generation of conditional knockout mice via sequential introduction of lox sites. *Sci. Rep.* **7**, 7891. <https://doi.org/10.1038/s41598-017-08496-8> (2017).
25. Team, R. R. *A language and environment for statistical computing*. <<https://www.R-project.org/>>
26. Lee, W. H., Michels, K. M. & Bondy, C. A. Localization of insulin-like growth factor binding protein-2 messenger RNA during postnatal brain development: Correlation with insulin-like growth factors I and II. *Neuroscience* **53**, 251–265. [https://doi.org/10.1016/0306-4522\(93\)90303-w](https://doi.org/10.1016/0306-4522(93)90303-w) (1993).
27. Bondy, C. & Lee, W. H. Correlation between insulin-like growth factor (IGF)-binding protein 5 and IGF-I gene expression during brain development. *J. Neurosci.* **13**, 5092–5104. <https://doi.org/10.1523/JNEUROSCI.13-12-05092.1993> (1993).
28. Khan, S. IGFBP-2 signaling in the brain: From brain development to higher order brain functions. *Front. Endocrinol.* **10**, 822. <https://doi.org/10.3389/fendo.2019.00822> (2019).
29. Tseng, L. Y. et al. The fetal rat binding protein for insulin-like growth factors is expressed in the choroid plexus and cerebrospinal fluid of adult rats. *Mol. Endocrinol.* **3**, 1559–1568. <https://doi.org/10.1210/mend-3-10-1559> (1989).

30. Garcia-Segura, L. M., Perez, J., Pons, S., Rejas, M. T. & Torres-Aleman, I. Localization of insulin-like growth factor I (IGF-I)-like immunoreactivity in the developing and adult rat brain. *Brain Res.* **560**, 167–174. [https://doi.org/10.1016/0006-8993\(91\)91228-s](https://doi.org/10.1016/0006-8993(91)91228-s) (1991).
31. Hales, C. N. & Barker, D. J. Type 2 (non-insulin-dependent) diabetes mellitus: The thrifty phenotype hypothesis. *Diabetologia* **35**, 595–601. <https://doi.org/10.1007/BF00400248> (1992).
32. Crowther, N. J., Cameron, N., Trusler, J. & Gray, I. P. Association between poor glucose tolerance and rapid post natal weight gain in seven-year-old children. *Diabetologia* **41**, 1163–1167. <https://doi.org/10.1007/s001250051046> (1998).
33. Carr, S. K. et al. Maternal diet amplifies the hepatic aging trajectory of Cidea in male mice and leads to the development of fatty liver. *FASEB J.* **28**, 2191–2201. <https://doi.org/10.1096/fj.13-242727> (2014).
34. Kwong, W. Y. et al. Imprinted gene expression in the rat embryo-fetal axis is altered in response to periconceptual maternal low protein diet. *Reproduction* **132**, 265–277. <https://doi.org/10.1530/rep.1.01038> (2006).
35. Kammel, A. et al. Early hypermethylation of hepatic Igfbp2 results in its reduced expression preceding fatty liver in mice. *Hum. Mol. Genet.* **25**, 2588–2599. <https://doi.org/10.1093/hmg/ddw121> (2016).
36. McDonald, K. L. et al. IQGAP1 and IGFBP2: Valuable biomarkers for determining prognosis in glioma patients. *J. Neuropathol. Exp. Neurol.* **66**, 405–417. <https://doi.org/10.1097/nen.0b013e31804567d7> (2007).
37. Zheng, S. et al. DNA hypermethylation profiles associated with glioma subtypes and EZH2 and IGF2BP2 mRNA expression. *Neuro Oncol.* **13**, 280–289. <https://doi.org/10.1093/neuonc/noq190> (2011).
38. Chouchani, E. T., Kazak, L. & Spiegelman, B. M. New advances in adaptive thermogenesis: UCP1 and beyond. *Cell Metab.* **29**, 27–37. <https://doi.org/10.1016/j.cmet.2018.11.002> (2019).
39. Hiraoka, Y. et al. Critical roles of nardilysin in the maintenance of body temperature homeostasis. *Nat. Commun.* **5**, 3224. <https://doi.org/10.1038/ncomms4224> (2014).
40. Al-Samerria, S. & Radovick, S. The role of insulin-like growth factor-1 (IGF-1) in the control of neuroendocrine regulation of growth. *Cells* **10**, 2664. <https://doi.org/10.3390/cells10102664> (2021).
41. Baker, J., Liu, J. P., Robertson, E. J. & Efstratiadis, A. Role of insulin-like growth factors in embryonic and postnatal growth. *Cell* **75**, 73–82 (1993).

Acknowledgements

We thank Dr. Michio Miyoshi for the experimental support, and Dr. Satoshi Koba and Dr. Kunio Kondoh for the advice to our study. We also thank the Tottori Bio Frontier, which managed by Tottori prefecture in Japan, for use of research equipment.

Author contributions

Y.Y., T.W. and T.Y.H. conceived the study; Y.Y. and K.N. conducted the experiments; Y.Y. and T.Y.H. analyzed and interpreted the data; Y.Y. and T.Y.H. drafted and wrote the manuscript. A.F. and K.M. provided *CaMK2a-Cre* mice; All authors reviewed the manuscript; T.Y.H. supervised and approved the manuscript.

Funding

This study was supported by MEXT/JSPS KAKENHI (Grant nos. 15K08207, 22K06055, 21K18269, and 23H00422) and AMED (Grant no. JP23gm1510001).

Declarations

Competing interests

The authors declare no competing interests.

Additional information

Supplementary Information The online version contains supplementary material available at <https://doi.org/10.1038/s41598-024-80252-1>.

Correspondence and requests for materials should be addressed to Y.Y. or T.Y.H.

Reprints and permissions information is available at www.nature.com/reprints.

Publisher's note Springer Nature remains neutral with regard to jurisdictional claims in published maps and institutional affiliations.

Open Access This article is licensed under a Creative Commons Attribution-NonCommercial-NoDerivatives 4.0 International License, which permits any non-commercial use, sharing, distribution and reproduction in any medium or format, as long as you give appropriate credit to the original author(s) and the source, provide a link to the Creative Commons licence, and indicate if you modified the licensed material. You do not have permission under this licence to share adapted material derived from this article or parts of it. The images or other third party material in this article are included in the article's Creative Commons licence, unless indicated otherwise in a credit line to the material. If material is not included in the article's Creative Commons licence and your intended use is not permitted by statutory regulation or exceeds the permitted use, you will need to obtain permission directly from the copyright holder. To view a copy of this licence, visit <http://creativecommons.org/licenses/by-nc-nd/4.0/>.

© The Author(s) 2024